Nagata patch interpolation for finite volume mechanical contact simulations

Ivan Batistić [1], Željko Tuković [1], Philip Cardiff [2], Peter De Jaeger [3]
Faculty of Mechanical Engineering and Naval Architecture, Zagreb, Croatia[1]
University College Dublin, School of Mechanical and Materials Engineering, Belfield, Ireland[2]
NV Bekaert SA, Belgium[3]
ivan.batistic@fsb.hr

Abstract: *This paper describes a finite volume contact algorithm with surface smoothing using the Nagata patch interpolation. Nagata interpolation is derived from existing discretisation, using the mesh points positions and their calculated normal vectors. The contact between a deformable and a rigid body is analysed, whereas the rigid body is described with Nagata patch interpolation. Such approach allows a more accurate evaluation of the resulting contact stresses and forces.*
Keywords*: MECHANICHAL CONTACT SIMULATION, SURFACE SMOOTHING METHOD, NAGATA PATCH INTERPOLATION, FINITE VOLUME METHOD, FOAM-EXTEND*

1. Introduction

As the finite element method is a common approach in the numerical stress analysis, it is also the most developed and advanced numerical method for calculating mechanical contact problems [1]. Recently, the finite volume method has established itself as a noteworthy alternative to the widely used finite element method in the simulation of stress analysis problems. Since the finite volume method proved to be capable of resolving strongly non-linear fluid flow problems, it is successfully applied to non-linear solid mechanics problems [2, 3].

Although the development and application of the finite volume method for stress analysis problems began more than two decades ago, the mechanical contact applications are still limited. The first finite volume mechanical contact calculation algorithm is proposed in [4] for linear elastic solids, where the contact constraint is enforced using the Dirichlet-Neumann partitioned procedure. The proposed Dirichlet-Neumann partitioned procedure was appropriate for two-dimensional cases, but it showed substantial limitations in three-dimensional applications, where it was difficult to prevent unphysical stresses at the edge of the contact surface. Because of the mentioned limitations, a contact algorithm based on the penalty method is developed in [5]. The proposed algorithm is based on the explicit update of contact force calculated at mesh points using penalty method. The calculated contact force is imposed on boundary via Neumman boundary condition. The algorithm was originally developed for three-dimensional frictionless problems. The extension on problems with friction and large elastoplastic deformation is done in [2]. The proposed contact calculation algorithm showed good stability and accuracy for complex contact problems. In order to better describe the friction in metal forming processes, the algorithm is extended to consider the lubrication in [6]. The lubrication is modelled by the Reynolds lubrication equations and solved numerically using the finite area method.

Algorithms for calculating contact problems with the finite element method cannot be directly applied to the finite volume method. In the finite element method, the weak form of the equation is solved. The contact effects are introduced via additional contact term in the energy functional. Furthermore, the solution is obtained by minimizing the modified energy functional [1] with methods well known in the optimization theory, where the constrained minimization problem is converted into an unconstrained saddle point problem. The most usable optimization methods in contact mechanics are the penalty method, the Lagrange multiplier method and the Augmented Lagrangian method [1]. In the finite volume method minimization of the energy is not carried out because a strong form of governing equations is discretized. Furthermore, the contact is treated like boundary conditions and the contact force is explicitly updated for each iteration of the segregated solver. It is important to notice that for both numerical methods, the algorithms for calculating contact problems are incremental and iterative since contact surfaces are unknown.

The purpose of this study is the development of the surface smoothing method for the finite volume contact algorithm. For the surface smoothing, Nagata patch interpolation is adopted to accurately describe contact surface. The main advantage of the chosen surface smoothing method is that it can be carried out efficiently and locally. The proposed procedure is implemented and tested in the foam-extend open source library.

2. Mathematical model

For each bodie in contact the conservation of linear momentum is considered:

$$\frac{\partial}{\partial t}\int_{\Omega}\rho\frac{\partial \boldsymbol{u}}{\partial t}\,\mathrm{d}\Omega = \oint_{\Gamma}\boldsymbol{n}\cdot\boldsymbol{\sigma}\,\mathrm{d}\Gamma + \int_{\Omega}\rho\boldsymbol{b}\,\mathrm{d}\Omega, \tag{1}$$

where ρ is the density, $\boldsymbol{u}$ is the displacement vector, $\boldsymbol{\sigma}$ is the Cauchy stress tensor, and $\boldsymbol{b}$ is a body force per mass unit. With appropriate constitutive equation for each bodie, the eq. (1) is reformulated into updated or total Lagrangian form. After the finite volume discretisation, a system of linear algebraic equations is obtained and solved in a segregated manner using iterative solvers. Contact is introduced via Neumann boundary condition, where the contact constraints are enforced using penalty method. More details about finite volume discretisation and solution procedure can be found in [2, 3].

2.1 Contact constraints

The mathematical background of the contact problem is defined by the contact constrains. The contact constraints can be divided into normal and tangential constraints. Accordingly, the normal contact constrains describe the normal component of the contact force, whereas the tangential constraints describe the tangential component of the contact force. The normal contact constraints are formulated using the Karush-Kuhn-Tucker conditions, being stated as:

$$g_n \geqslant 0, \quad p_n \leqslant 0, \quad p_n g_n = 0, \tag{2}$$

which must hold for all points on contact surface. The first term in the eq. (2) represents the geometric impenetrability condition. The second term allows only compressive contact pressure p_n, whereas the third term is the complementarity condition. Tangential contact constraints are described by a friction law. Most famous and simplest friction law is Coulomb law, which is described by the following three conditions:

$$\|\boldsymbol{t}_t\| - \mu|p_n| \leqslant 0, \;\; t_t + \mu|p_n|\frac{\dot{\boldsymbol{g}}_t}{\|\dot{\boldsymbol{g}}_t\|} = 0, \;\; \|\dot{\boldsymbol{g}}_t\|\left(\|\boldsymbol{t}_t\| - \mu|p_n|\right) = 0, \tag{3}$$

where μ is the constant friction coefficient, $\dot{\boldsymbol{g}}_t$ tangential relative sliding velocity and $\boldsymbol{t}_t$ the frictional force vector. The first term in eq. (3) limits the frictional contact force, the second term defines its direction, whereas the third term is the complementarity condition. To conclude, the contact conditions, i.e. components of contact force, are described by nonlinear functions. Hence, they are the main source of the nonlinearity of contact problems.

3. Surface smoothing method

From the numerical point of view, the finite volume analysis of contact problems can be divided into two categories. First, the general category represents contact between deformable discretized bodies whereas the second category is the simplification in which one bodie is rigid. For contact problems with large difference between stiffness of the contact bodies, the stiffer bodie can be represented as a rigid. Such approach leads to less computational effort and can be used in the simulations of complex engineering problems like: metal forming processes, rubber seals, tyre on road, indentation tests [7, 8, 9]. The representation of rigid body surface can be done using analytical surfaces, piecewise linear discretisation or with parametric patches obtained with surface smoothing. The analytical approach is limited on simpler geometry, whereas piecewise discretisation poses some drawbacks when point projection is calculated. Using surface smoothing methods, rigid contact surface is accurately and continuously described using higher order interpolations. Although, various surface smoothing methods have been developed in the finite element method, the recently applied Nagata patch interpolation can be easily generalized and efficiently applied on arbitrary piecewise linear finite volume mesh topology.

3.1 Nagata patch interpolation

The Nagata patch interpolation was originally proposed by Nagata [10]. The interpolation is based on a quadratic polynomial, requiring only position and normal vectors at the nodes of the surface mesh. The features of the proposed interpolation algorithm allows its efficient and robust application on arbitrary mesh topology. It is important to note that the proposed formulation can handle discontinuity of normals, sharp edges and singular points. In the presented study the interpolation method is used on smooth rigid surfaces, discretized with triangular facets.

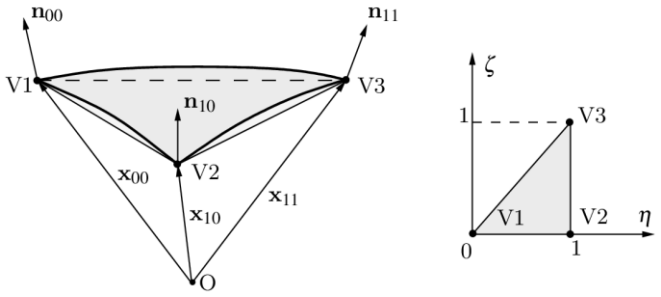

Fig. 1 *Nagata patch interpolation.*

For triangular Nagata patch (see Fig.1), the interpolated surface is given by the quadratic polynomial:

$$\boldsymbol{x}(\eta,\zeta)=\boldsymbol{c}_{00}+\boldsymbol{c}_{10}\eta+\boldsymbol{c}_{01}\zeta+\boldsymbol{c}_{11}\eta\zeta+\boldsymbol{c}_{20}\eta^2+\boldsymbol{c}_{02}\zeta^2, \qquad (4)$$

where η and ζ are the local coordinates defined on the patch region, and satisfy the next condition:

$$0\leqslant\zeta\leqslant\eta\leqslant 1. \qquad (5)$$

The coefficients in equation (4) are:

$$\begin{gathered}\boldsymbol{c}_{00}=\boldsymbol{x}_{00},\quad \boldsymbol{c}_{10}=\boldsymbol{x}_{10}-\boldsymbol{x}_{00}-\boldsymbol{c}_1,\quad \boldsymbol{c}_{01}=\boldsymbol{x}_{11}-\boldsymbol{x}_{10}+\boldsymbol{c}_1-\boldsymbol{c}_3\\ \boldsymbol{c}_{11}=\boldsymbol{c}_3-\boldsymbol{c}_1-\boldsymbol{c}_2,\quad \boldsymbol{c}_{20}=\boldsymbol{c}_1,\quad \boldsymbol{c}_{02}=\boldsymbol{c}_2,\end{gathered} \qquad (6)$$

where $\boldsymbol{c}_1$, $\boldsymbol{c}_2$ and $\boldsymbol{c}_3$ are the vectors obtained with the edge interpolation. For each edge ($\boldsymbol{x}_{00}$, $\boldsymbol{x}_{10}$), ($\boldsymbol{x}_{10}$, $\boldsymbol{x}_{11}$) and ($\boldsymbol{x}_{00}$, $\boldsymbol{x}_{11}$), quadratic Nagata curve can be defined (see Fig. 2):

$$\boldsymbol{x}(\zeta)=\boldsymbol{x}_1+(\boldsymbol{x}_2-\boldsymbol{x}_1-\boldsymbol{c})\zeta+\boldsymbol{c}\zeta^2 \quad \text{where } 0\leqslant\zeta\leqslant 1. \qquad (7)$$

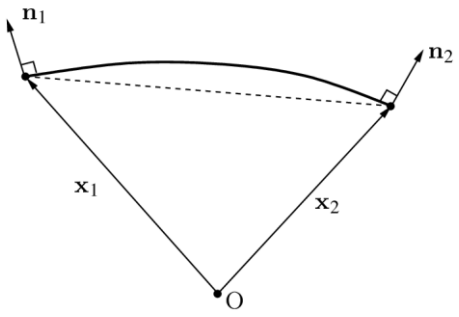

Fig. 2 *Nagata edge curve*

Vectors $\boldsymbol{x}_1$ and $\boldsymbol{x}_2$ are the position vectors of the edge end points, and $\boldsymbol{c}$ is the unknown coefficient vector. Coefficient vector c is calculated as:

$$\boldsymbol{c}=\begin{cases}\dfrac{[\boldsymbol{n}_1,\boldsymbol{n}_2]}{1-a^2}\begin{bmatrix}1 & -a\\ -a & 1\end{bmatrix}\begin{Bmatrix}\boldsymbol{n}_1\cdot(\boldsymbol{x}_2-\boldsymbol{x}_1)\\ -\boldsymbol{n}_2\cdot(\boldsymbol{x}_2-\boldsymbol{x}_1)\end{Bmatrix} & (a\neq\pm1)\\ 0 & (a=\pm1)\end{cases}, \qquad (8)$$

where $a=\mathbf{n}_1\cdot\mathbf{n}_2$ and $[\cdot,\cdot]$ represent a matrix composed by two vectors. Equation (8) is derived from the assumption that the Nagata curve is orthogonal to the unit normal vectors $\boldsymbol{n}_1$ and $\boldsymbol{n}_2$ at points $\boldsymbol{x}_1$ and $\boldsymbol{x}_2$, respectively. For the parallel normal vectors ($a=\pm1$), the Nagata curve describes the linear segment, because of the zero coefficient vector $\boldsymbol{c}$. More details about the Nagata patch interpolation on triangular and quadrilateral patch can be found in the literature [11, 12].

3.2 Point normal calculation

In order to construct the Nagata patch, the calculation of normals at mesh vertices is conducted. The normal vectors at mesh points are estimated with normals from the point neighbouring faces. The calculation is done using the weighted average of the unit normal vectors of all neighbouring faces:

$$\boldsymbol{n}_{\mathrm{p}}=\frac{\sum_{i=1}^{n_f}\omega_i\boldsymbol{n}_{f,i}}{\left\|\sum_{i=1}^{n_f}\omega_i\boldsymbol{n}_{f,i}\right\|}. \qquad (9)$$

In the presented study each neighbouring face contributes equally to the normal vector calculation (mean weighted equally). In the literature more advanced approach can be found, such as mean weighted by angle or mean weighted by areas of adjacent triangles [12].

4. Contact algorithm

The first part of the contact algorithm is the contact search. For each mesh point $\boldsymbol{P}$ of the deformable body potential Nagata contact candidates are identified. The potential contact candidates are calculated using the Axis Aligned Bounding Box quick rejection test. Such approach generates false candidates which are detected and eliminated using the Separation Axis Theorem algorithm. Using potential candidate list, for each contact point, the closest point projection is calculated for all candidates in order to find the minimal normal gap value. The relationship between the coordinates of contact point and closest point on Nagata patch is described with the following equation:

$$F^{\mathrm{proj}}(\eta,\zeta,g_n)=\boldsymbol{x}(\eta,\zeta)+g_n\boldsymbol{n}(\eta,\zeta)-\boldsymbol{P}=0, \qquad (10)$$

where $\boldsymbol{P}$ denotes the contact point on the deformable contact surface, $\boldsymbol{x}$ closest point on the Nagata patch and $\boldsymbol{n}$ unit normal vector of the Nagata patch (see Fig 2). The patch normal vector is calculated as follows:

$$\boldsymbol{n}=\frac{\boldsymbol{t}_1\times\boldsymbol{t}_2}{\|\boldsymbol{t}_1\times\boldsymbol{t}_2\|}, \qquad (11)$$

where $\boldsymbol{t}_1$ and $\boldsymbol{t}_2$ are surface tangents at point $\boldsymbol{x}(\eta, \zeta)$, defined as:

$$\begin{aligned}\boldsymbol{t}_1&=\frac{\partial \boldsymbol{x}}{\partial \eta}=\boldsymbol{x}_{10}-\boldsymbol{x}_{00}+\boldsymbol{c}_1\left(\left(\eta-\zeta\right)-\left(1-\eta\right)\right)+\left(\boldsymbol{c}_3-\boldsymbol{c}_2\right)\zeta,\\ \boldsymbol{t}_2&=\frac{\partial \boldsymbol{x}}{\partial \zeta}=\boldsymbol{x}_{11}-\boldsymbol{x}_{10}+\boldsymbol{c}_2\left(\zeta-\left(\eta-\zeta\right)\right)+\left(\boldsymbol{c}_1-\boldsymbol{c}_3\right)\left(1-\eta\right).\end{aligned} \tag{12}$$

The solution of $\boldsymbol{F}^{\text{proj}} = 0$ provides the local coordinate of the closest point $\bar{\boldsymbol{x}}$ on the Nagata patch. In order to solve the eq. (10) the Newton-Raphson method is used:

$$\boldsymbol{s}_{i+1}=\boldsymbol{s}_i-\left[\nabla \boldsymbol{F}^{\text{proj}}\left(\boldsymbol{s}_i\right)\right]\boldsymbol{F}^{\text{proj}}\left(\boldsymbol{s}_i\right), \tag{13}$$

where $\boldsymbol{s}_i=[\eta, \zeta, g_n]^T$ represents the solution vector at iteration i. The Jacobian matrix $\nabla \boldsymbol{F}^{\text{proj}}$ of the system of equations in the eq. (13) is defined as follows:

$$\nabla \boldsymbol{F}^{\text{proj}}\left(\eta,\zeta,g_n\right)=\left[\frac{\partial}{\partial \eta},\frac{\partial}{\partial \zeta},\frac{\partial}{\partial g_n}\right]\boldsymbol{F}^{\text{proj}}\left(\eta,\zeta,g_n\right). \tag{14}$$

In order to calculate the eq. (14) the gradient of the normal vector with respect to the local coordinates is evaluated using the Weingarten formula.

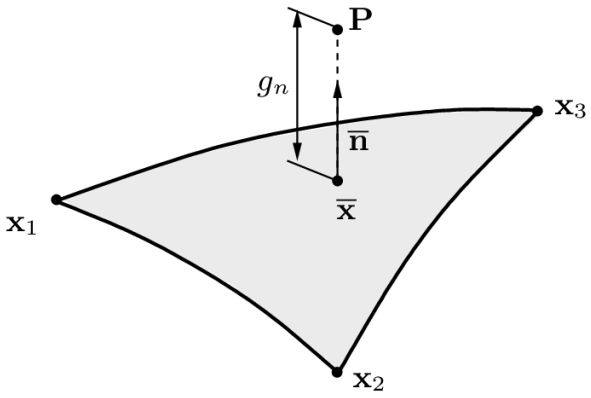

Fig. 3 *Closest point projection.*

For most cases solution of the eq. (13) is obtained with less than four iterations. With the obtained normal gap at mesh points, normal contact pressure is calculated using the penalty method, whereas the value at face center is obtained using the inverse distance interpolation.

2. Numerical examples

The proposed contact algorithm is implemented in the open-source foam-extend library as the extension to the work previously done by [2, 5]. The accuracy and efficiency of the proposed contact algorithm are tested via two numerical examples. The first example is a simple two-dimensional example of compressed cylinder tube with an exterior rigid tube. The second case is the finite element benchmark case initially proposed by Krstulović-Opara [13]. The examinated numerical examples comprise frictional and frictionless contact between rigid and deformable body, whereas the deformable body includes large deformation and large sliding. In both numerical examples, the Neo-Hookean material model is chosen for the deformable body. The results are compared with the current finite volume contact algorithm [2, 5], where the piecewise linear surface description is used.

5.1 Compressing cylindrical tube

Elastic cylindrical tube (Young's modulus E = 200 MPa, Poisson's ration υ = 0.3) with inner radius r_i =50 mm and thickness 15 mm, is initially overlapped δ= 1mm with exterior rigid cylindrical tube. Due to the symmetry of the problem, only 1/4 of the model is considered, which is discretized with 10 cells in radial and 40 cells in a circular direction. Rigid cylinder tube is discretised with two meshes (see Fig. 4), whereas mesh A consists of the same number of faces in the circular direction, resulting in accurate calculation of the normal gap at mesh points. At the contact interface, frictionless contact is assumed. From the Fig. 5 it can be seen that non-conformal discretisation on the contact interface produces stress oscillations, whereas application of surface smoothing produces results with a smooth distribution of radial stress.

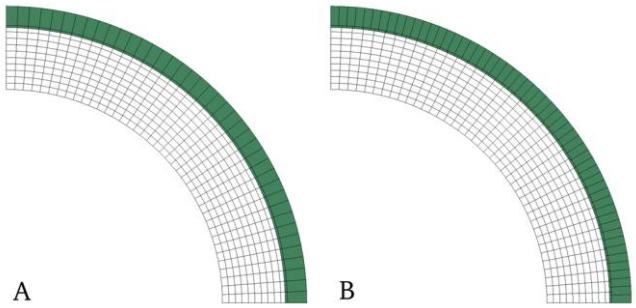

Fig. 4 *Cylindrical tube mesh: a) conformal, b) non-conformal discretisation at the contact interface.*

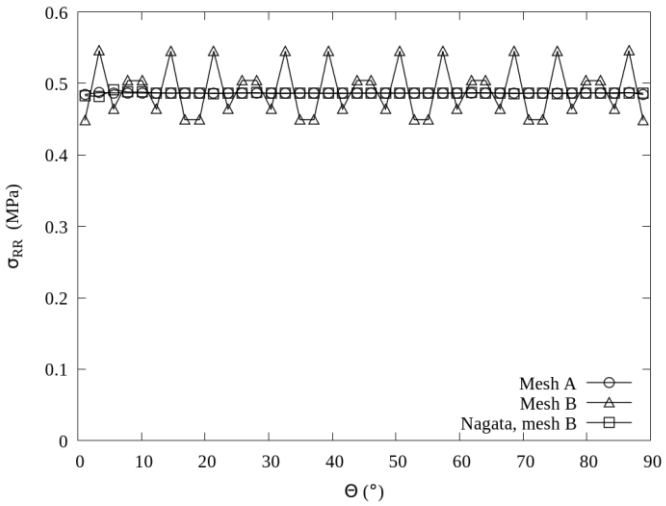

Fig. 5 *Radial stress distribution on the contact surface.*

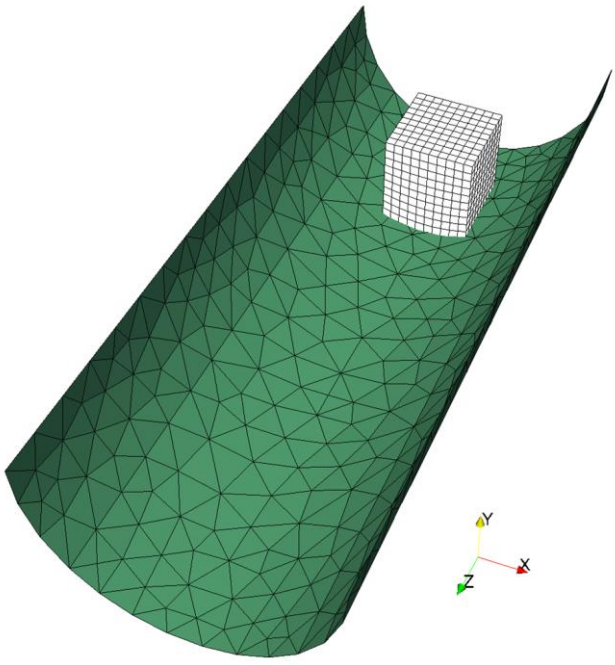

Fig. 6 *Unstructured mesh of a half-tube, 580 triangles (mesh A).*

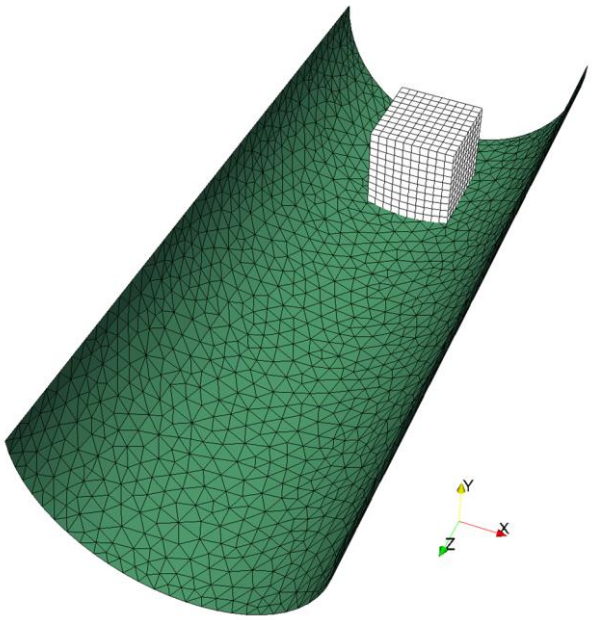

Fig. 7 *Unstructured mesh of a half-tube, 2442 triangles (mesh B).*

5.2 Cylindrical contactor sliding in a half-tube

This case represents the sliding of an elastic cylindrical contactor in a rigid tube. The cylindrical contractor dimensions are 2×2×2 with the curvature radius r=3 in the contact surface. The half-tube has a radius of r=3 and 15 units of length. The Young's modulus and the Poisson's ratio are defined as E=100 and υ=0.3, respectively. The friction is described with Coulomb friction law with coefficient of friction μ=0.1. The cylindrical contractor is uniformly discretized with 100 control volumes, whereas the rigid half-tube is discretized with unstructured mesh composed by 580 and 2442 triangles (see Fig. 6 and Fig. 7). At initial configuration the cylinder contactor overlaps rigid tube by δ=0.01 units. The axial displacement of 10 units in z direction is prescribed and solved via 100 equal increments. From Fig. 8 it is possible to conclude that coarse discretisation leads to bad force evolution because of the poor approximation of the cylinder surface geometry. Furthermore, finer discretisation produces results closer to ones obtained using surface smoothing. It is important to notice that the application of surface smoothing leads to approximately the same force evolution on both meshes studied. In this example, the average number of iterations per timestep is decreased for both meshes when mesh smoothing is used. Obtained results are in good agreement with [11] where the finite element method is used.

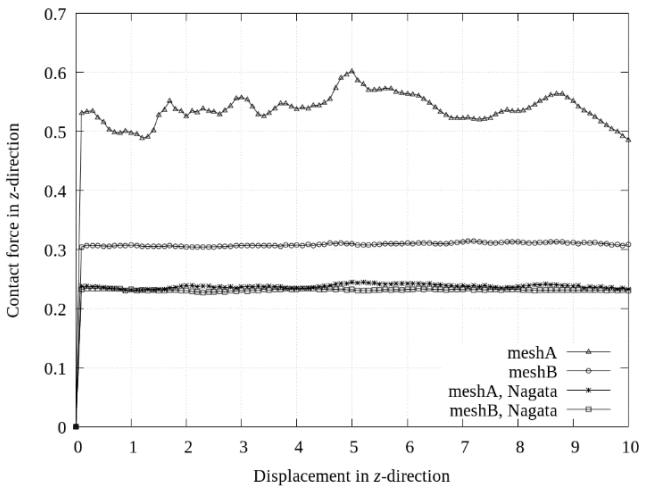

Fig. 8 *Comparison of the contact force as a function of displacement for piecewise linear and the smooth surface description of the half-tube.*

6. Conclusion

A patch smoothing procedure for the finite volume mechanical contact simulations is presented in this work. The implementation is done in the foam-extend framework, as the extension of the existing code developed for large deformation contact problems [2, 5]. The results are compared with the existing finite volume contact algorithm via two numerical examples. The results show that the Nagata patch interpolation allows more accurate evaluation of contact stresses. Furthermore, because of the continuous description of boundary, the force oscillations are reduced. For the future work, the efficiency and robustness of the current implementation will be tested and presented. Moreover, the implementation will be extended to handle the contact between deformable bodies.

7. Acknowledgements

Financial support via Ph.D. funding is gratefully acknowledged from NV Bekaert SA, Belgium.

8. References

1. P. Wriggers, Computational Contact Mechanics. Springer, **2**nd edition, (2006).
2. P. Cardiff, Ž. Tuković, P. DeJaeger, M. Clancy, A. Ivanković, A Lagrangian cell-centred finite volume method for metal forming simulation, International Journal for Numerical Methods in Engineering, **109(13)**, 1777-1803, (2017) .
3. Ž. Tuković, A. Karač, P. Cardiff, H. Jasak and A. Ivanković, OpenFOAM finite volume solver for fluid-solid interaction. Transactions of FAMENA, **42(3)**, pp.1-31, 2018.
4. H. Jasak, H. Weller, Finite Volume Methodology for Contact Problems of Linear Elastic Solids, Proceedings of 3rd International Conference of Croatian Society of Mechanics, Cavtat/Dubrovnik, 253-260, (2000).
5. P. Cardiff, A. Karač, A. Ivanković. Development of a finite volume contact solver based on the penalty method, Computational Materials Science, 283-284, (2012).
6. V. Škurić, P. De Jaeger and H. Jasak, Lubricated elastoplastic contact model for metal forming processes in OpenFOAM. Computers & Fluids, **172**, pp.226-240, (2018).
7. D. M. Neto, M. C. Oliveira, and L. F. Menezes, Surface smoothing procedures in computational contact mechanics, Archives of Computational Methods in Engineering **24.1,** 37-87, (2017).
8. M. Hachani and L. Fourment, 3D contact smoothing method based on Quasi-C1 interpolation, Trends in computational contact mechanics, **58**, 23-40, (2011).
9. T. Hama, T. Nagata, C. Teodosiu, A. Makinouchi and H. Takuda, Finite-element simulation of springback in sheet metal forming using local interpolation for tool surfaces. International Journal of Mechanical Sciences, **50(2)**, 175-192, (2008).
10. T. Nagata, Simple local interpolation of surfaces using normal vectors, Computer Aided Geometric Design, **22**, 327-347, (2005).
11. D. M. Neto, M. C. Oliveira, L. F. Menezes and J. L. Alves, Applying Nagata patches to smooth discretized surfaces used in 3D frictional contact problems, Computer Methods in Applied Mechanics and Engineering, **271**, 296-320, (2014).
12. D. M. Neto, M. C. Oliveira, L. F. Menezes and J. L. Alves, A contact smoothing method for arbitrary surface meshes using Nagata patches, Computer Methods in Applied Mechanics and Engineering **299,** 283-315, (2016).
13. L. Krstulović-Opara, P. Wriggers, and J. Korelc, AC 1-continuous formulation for 3D finite deformation frictional contact, Computational Mechanics, **29.1**, 27-42, (2002).